Chinese Chemical Letters 33 (2022) 1850–1854

Contents lists available at ScienceDirect

Chinese Chemical Letters

journal homepage: www.elsevier.com/locate/cclet

Highly fluorescence Ta_4C_3 MXene quantum dots as fluorescent nanoprobe for heavy ion detection and stress monitoring of fluorescent hydrogels

Shouzhen Li[a,1], Junfei Ma[a,1], Xuelin Zhao[b,1], Peide Zhu[a], Meng Xu[b], Yingchun Niu[a,*], Dixian Luo[c,*], Quan Xu[a,*]

[a] State Key Laboratory of Shale Oil and Gas Enrichment Mechanisms and Effective Development, National Energy Shale Oil Research and Development Center, China University of Petroleum (Beijing), Beijing 102249, China
[b] Department of Musculoskeletal Tumor, Senior Department of Orthopedics, the Fourth Medical Center of PLA General Hospital, Beijing 100142, China
[c] Department of Laboratory Medicine, Huazhong University of Science and Technology Union Shenzhen Hospital (Nanshan Hospital), Shenzhen 518000, China

ARTICLE INFO

Article history:
Received 24 August 2021
Revised 29 October 2021
Accepted 3 November 2021
Available online 11 November 2021

Keywords:
MXene quantum dots
Fluorescent probe
Fluorescent hydrogel
Hydrothermal method
Quantum yield

ABSTRACT

Compared with other transition metal Mxene derived quantum dots (MQD_S), Ta-based Mxene quantum dots have good functionality, but Ta-based Mxene quantum dots and their applications have not been studied so far. In this paper, we report for the first time the synthesis of high fluorescence quantum yield (QY) N-doped Ta_4C_3 quantum dots (N-MQDs) using Ta_4C_3 quantum dots in acid reflux damaged Ta_4C_3 nanosheets as precursors and ethylenediamine as nitrogen source. The prepared N-MQDs have excellent blue photoluminescence (PL) properties, particle size is only 2.60 nm, QY is up to 23.4%, and good stability. In addition, it has been reported that N-MQDs can be used as fluorescent probe for detection of Fe^{3+} and remote force sensing analysis In liquid ion sensing, N-MQDS shows a unique selective quenching of Fe^{3+} with a detection limit as low as 2 μmol/L, and has great potential as a fast and super-sensitive fluorescent probe for the detection of heavy ion. More importantly, in solid mechanics sensing, the introduction of N-MQDs into self-healing hydrogels can be developed into a fluorescent hydrogel that can be used for accurate remote force measurement and applied in the field of mechanical sensing analysis. Therefore, Ta-based N-MQDs show excellent potential in the field of fluorescence sensing, which provides a door for multi-dimensional sensing of new materials in the future.

Recently, two-dimensional (2D) Mxene as a new nanomaterial has been gradually developed, and shows excellent electro-optical, thermal and mechanical properties [1–3]. MXene is a novel two-dimensional layered material, which is the general name of transition metal-carbon and/or nitrite. The hydrophilic surface ends and transition metal elements give MXene excellent high conductivity, excellent hydrophilicity, superior thermal stability, large interlayer space, and high surface area [4,5]. Accordingly, MXene has great potential as a sensor device, but the low PL reaction of this material in solution has greatly limited its wide application. By doping heterogeneous elements (N, P, S, *etc.*), the optical properties and other chemical properties of nanomaterials such as MQDs can be effectively improved, such as the increase of QY, to expand their applications in environmental monitoring, fluorescence imaging, photosynthetic cell, photoelectric devices and other fields [6,7]. In previous studies, researchers have successfully prepared MQDs with high QY, such as Ti_3C_2, Mo_2C, Nb_2C, and explored their applications in environmental monitoring and electrical energy fields, Compared with other transition metal Mxene derived quantum dots (MQDS), Ta-based Mxene quantum dots have good functionality and excellent environmental friendliness compared with other Mxene quantum dots, but Ta_4C_3 MQDs and their application are still in the gap [8–12].

In this paper, we reported for the first time an excellent N-doped Ta_4C_3 quantum dots (N-MQDs), using the sensitivity of N-MQDs fluorescent probe to Fe^{3+} to detect the environment, such as heavy oil ion detection, which can promote the sustainable utilization of oil products, find oil problems in time and avoid risks. At the same time, the pressure sensing properties of fluorescent hydrogels provide the possibility for future applications of optical pressure detection [13–16].

* Corresponding authors.
E-mail addresses: ycniu92@163.com (Y. Niu), luodixian_2@163.com (D. Luo), xuquan@cup.edu.cn (Q. Xu).
[1] These authors contributed equally to this work.

https://doi.org/10.1016/j.cclet.2021.11.020
1001-8417/

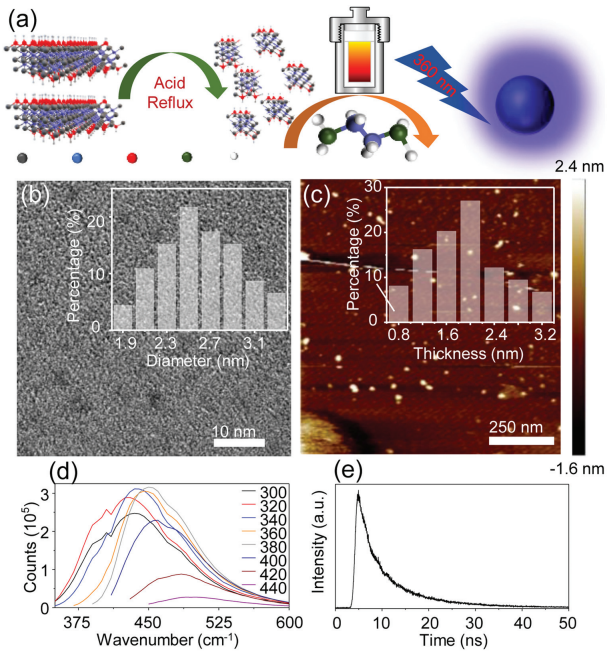

Fig. 1. (a) Schematic of preparation and light-emitting mechanism of the N-MQDs; (b) TEM image, inset: diameter size distribution; (c) AFM image of the N-MQDs, inset (top-right): thickness distribution of the N-MQDs; (d) Fluorescence emission spectra of the prepared N-MQDs (160 °C) at different excitation wavelengths (nm); (e) Fluorescence lifetime of N-MQDs.

The preparation of N-MQDs was in a typical process, and its synthesis scheme is illustrated in Fig. 1a. The structure of Ta_4C_3 was further studied, and the diameter information of N-MQDs was obtained by TEM, as showed in Fig. 1b. The diameter of N-MQDs is evenly distributed between 1.9–3.3 nm, with an average diameter of 2.60 nm, indicating that the N-MQDs are uniform in water and well separated. AFM image shows that the diameter of N-MQDs is evenly distributed between 0.8–3.2 nm (Fig. 1c), and the average thickness is 1.90 nm (Fig. S1 in Supporting information), the quasi spherical structure of MQDs also indirectly proves that N-MQD has been successfully synthesized [17,18]. Fig. 1d shows the fluorescence spectrum of N-MQDs. When the λ_{ex} (300–450 nm) of the N-MQDs changes, only the λ_{em} intensity decreases, while the peak position hardly changes, which indicates the emission excitation-dependent characteristics of the prepared N-MQDs. This excitation-dependent characteristic is believed to be related to the optical selection of different surface emission traps in N-MQDs nanoparticles of different sizes. The prepared N-MQD has a bright blue fluorescence at 450 nm (λ_{em}) when excited at 380 nm (λ_{ex}), and has bright blue fluorescence. In addition, we also explored the influence of different synthesis temperatures (120, 140, 160, 180, 200 °C) on the fluorescence intensity of N-MQDs. Experimental results prove that N-MQDs have the highest QY and fluorescence lifetime (Table S1 and Fig. S2 in Supporting information) at a hydrothermal temperature of 160 °C, it is noteworthy that both QY and fluorescence lifetime show a trend of first increasing and then decreasing with temperature. This may be because temperature affects the carbonization of N-MQDs, leading to differences in optical properties [1,17]. Fig. 1e is the PL lifetime decay curve, with a lifetime of 7.92 ns.

We also explored the effects of exposure time, temperature, and pH of aqueous solution to the fluorescence intensity of N-MQDs (Fig. S3 in Supporting information). The experimental results showed that the fluorescence emission intensity did not change significantly with the increase of the solution temperature, remained relatively stable. When the pH of an aqueous solution goes from 2 to 13, PL strength basically has no significant change. At the same time, the wavelength position and intensity of the fluorescence and absorption of N-MQDs show appropriate light-emitting time stability [18]. These results indicate that N-MQDs can be used in different environments, this excellent temperature and pH stability make the N-MQDs can be widely used in groundwater, unconventional oil and gas development, hydraulic fracturing and other fields [19].

Fig. 2a shows the UV–visible (UV–vis) absorption spectrum of the synthesized N-MQDs under UV irradiation at 360 nm, and absorption peaks are located at 234 and 293 nm, respectively. The strong absorption peak at 234 nm corresponds to π-π^* conjugate, and the other absorption peak found at 293 nm corresponds to n-π^* conjugate [17]. Fourier transform infrared spectroscopy (FTIR) was used to analyze the structure, composition and chemical bonds of the synthesized N-MQDs (Fig. 2b). It can be seen from the infrared spectrum that MQDs and N-MQDs have the constant vibration peaks. The peak at 3438 cm^{-1} is attributable to -OH and -NH groups. The single peak at 1650 cm^{-1} corresponds to the C=O stretching vibration. The peak at 1345 cm^{-1} is caused by -NH_2 vibration, and the intensity of N-MQDs is greater than that of MQDs, which proves the successful doping of N element on MQDs [20]. The peak of the C-O-C bond is located at 1092 cm^{-1} [21]. The peak at 943 cm^{-1} belongs to the Ta=O bond in the OTaCO group [23], especially the peak at 826 cm^{-1} may be explained by the vibration of the Ta-O bond. Infrared spectroscopy results show that the -NH group forms a passive surface on the N-MQDs, which makes the MQDs have excellent stability at different pH values and different temperatures. The surface modification of nanomaterials by hydroxyl and carbonyl groups makes the functionalized nanomaterials have good light stability [23].

X-ray diffraction (XRD) (Fig. 2c) was used to study the elemental composition and overall crystal structure of the original Ta_4C_3 MXene, MQDs and N-MQDs. The etched Ta_4C_3 MXene nanosheets have obvious (002), (015) and (018) peaks [24], which indicates that Ta_4C_3 MXene has a 2D layered structure. The peaks of N-MQDs contained the same peaks as Ta_4C_3 MXene, indicating that the prepared N-MQDs maintained the two-dimensional layered structure of the parent MXene material. It should be noted that there is a peak at 59.03°, which corresponds to the formation of impurity TaO. Due to the doping of heterogeneous elements, the angle of the (018) peak of the synthesized MQDs is slightly changed compared with that of the original Ta_4C_3 Mxene [25,26]. The element composition and valence state of N-MQDs were characterized and analyzed by X-ray Photoelectron Spectroscopy (XPS) (Figs. 2d-h). The contents of C, N, O and Ta elements in the samples were analyzed by XPS, and the high-resolution XPS spectra of MQDs and Ta_4C_3 was compared to indicates the successful doping of N element (Table S2 and Fig. S4 in Supporting information). XPS was used to identify the properties of chemical bonds in the C 1s, O 1s, N 1s and Ta 4f regions of the sample. The results show that N-MQDs have a 2D layered structure consistent with the parent MXene. The XPS spectrum of N-MQDs (Fig. 2d) all showed 4 peaks, which are 285.08, 535.08, 400.08 and 30.08 eV, corresponding to C 1s, O 1s, N 1s and Ta 4f [22,27], respectively. In the high-resolution C 1s spectrum (Fig. 2e), the C 1s XPS spectrum of N-MQDs shows four peaks at 283.3, 284.8, 285.5 and 288.3 eV [19]. The peak centered at 283.3 eV in the XPS spectrum of N-MQDs corresponds to the Ta-C_x bond. The peak of 284.8 eV corresponds to the C-C bond that may be formed during the synthesis of MXene. The "graphitized" nitrogen (C-N-H) bond corresponds to the peak of 285.5 eV, and the existence of the C-N bond is consistent with the results of FTIR (Fig. 2b) [28,29]. The peak centered at 288.3 eV corresponds to the C=O bond. The O 1s XPS spectrum of N-MQDs (Fig. 2f) forms four peaks at 530.9, 531.8, 533.0 and 535.4 eV, corresponding to TaC_x

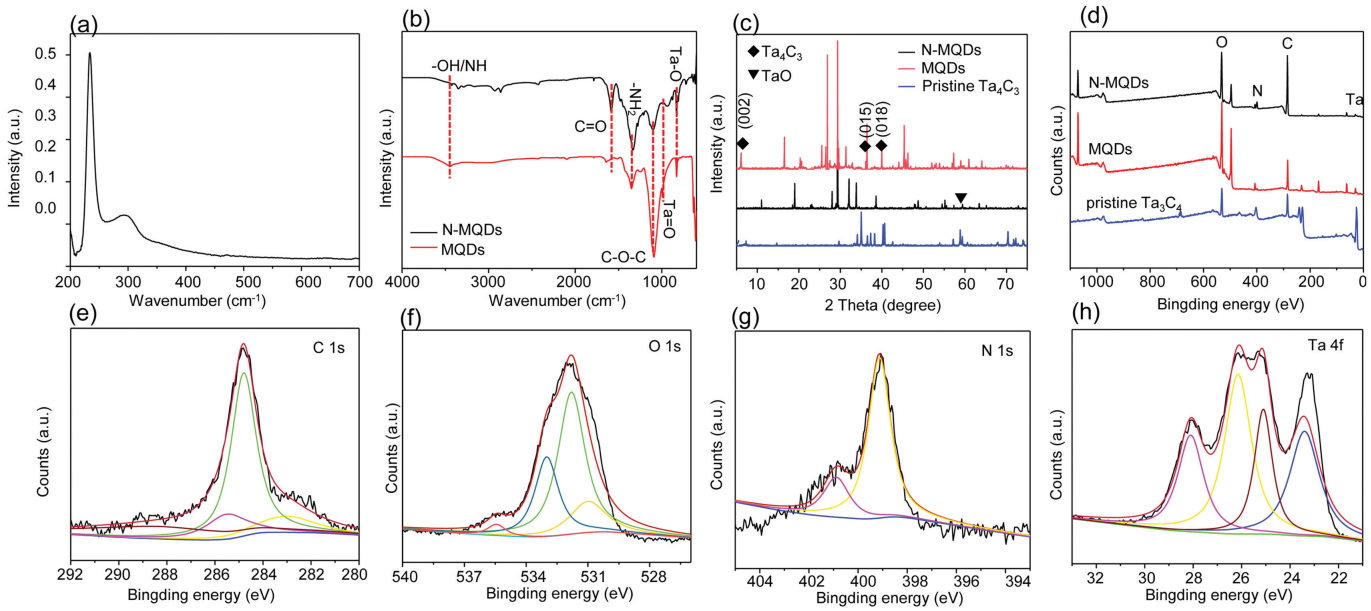

Fig. 2. (a) UV–vis absorption; (b) FTIR spectra; (c) XRD spectra of pristine MQDs, N-MQDs and pristine Ta_4C_3 MXene; (d) XPS survey spectra, high-resolution XPS spectra of (e) C 1s, (f) O 1s, (g) N 1s, (h) Ta 4f.

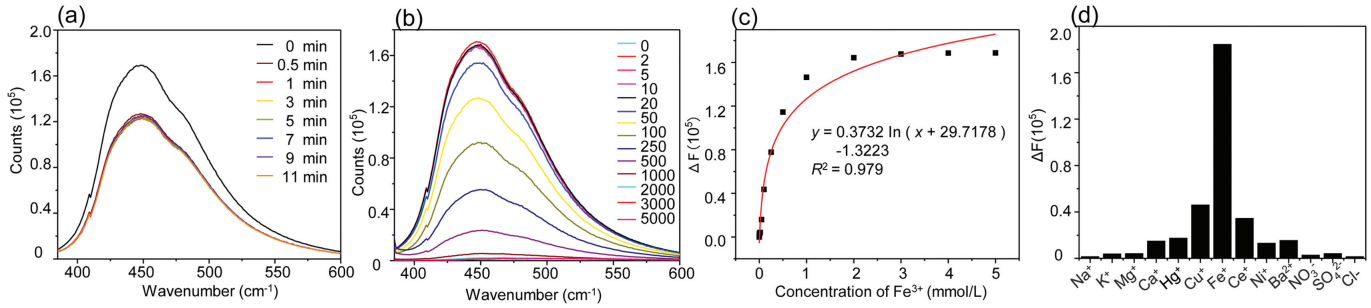

Fig. 3. (a) Time-dependent fluorescence changes of the N-MQDs in the presence of Fe^{3+} (100 μmol/L); (b) PL emission spectra of the Fe^{3+} (N-MQDs) solution with different concentrations (μmol/L) of Fe^{3+}; (c) The ΔF calibration curve of the N-MQDs solution *versus* the concentration of Fe^{3+}; (d) The ΔF at 370 nm for N-MQDs in the presence of various metal ions (100 μmol/L).

(-O end), $Ta_4C_3(OH)_x$ (-OH end), $Ta_4C_3(OH)_x$-H_2O_{ads} (the -OH end strongly adsorbs water) and C-OH bond, respectively. This corresponds to the typical surface end -O, -OH and -F of Ta_4C_3 Mxenes [29]. The -OH bond indicates that the N-MQDs are connected by hydrogen bonds on the surface, which leads to the fixation of C=O and C-O bonds, which greatly enhances the entire system's stability. The two peaks formed by the high-resolution N 1s spectrum (Fig. 2g) at 400.8 and 399.1 eV correspond to the nitrogen ($-NH_2$) and pyrrole-like nitrogen (C-N) in the amine group, indicating that the functionalized nitrogen is $-NH_2$ and C-N The form of bond is doped into N-MQDs. In the presence of pyrrole-like nitrogen, N doping tends to occur at the position where the defective bond shrinks, and pentagonal rings also appear at the position where the defective bond shrinks more. The high-resolution Ta 4f spectrum was used to characterize the bonding configuration of nitrogen atoms in N-MQDs (Fig. 2h). The Ta 4f spectrum contains four peaks at 23.4, 25.1, 26.1, and 28.1 eV. The peak at 23.4 eV corresponds to $4f_{7/2}$ sites of TaC_x, the peak at 25.1 eV corresponds to $4f_{5/2}$ sites of TaC_x, and the peak at 163.94 eV is accredited to the $4f_{7/2}$ sites of $[N(C_2H_5)_4]_2[Ta_6Cl_{12}Cl_6]$, the peak at 28.1 eV corresponds to $4f_{5/2}$ sites Ta_2O_5 [27,30,31]. The results show N elements are successfully doped into the MQDs. It is worth seeing that there is a uniform displacement of binding energy, which further proves the chemical bond interaction between N and other elements, and better proves that N has been successfully doped into MQDs. Thanks to the surface of N-MQDs is rich in $-NH_2$, -OH and other groups as well as N and O, it has a strong electron-absorbing ability and can effectively passivate the active sites on the surface. And quantum binding and edge effect of N-MQDs, it is useful to improve the stability and fluorescence performance of MQDs [32,33]. The results show that N-MQD is functionalized by N atoms, and the emission and corresponding fluorescence properties of quantum dots are improved, such as PLQY, which provides an idea for the subsequent adjustment of Ta_4C_3 Mxene.

Based on the excellent QY properties of N-MQDs, we explored the application of N-MQDs in fluorescent probes [34–37]. Fe^{3+} is very important in both biological environment and natural environment. Fe^{3+} is the core part of hemoglobin and an indispensable substance in various physiological processes. At the same time, Fe^{3+} is the key index of oil quality in the process of oil production [37–39]. We detected the effect of N-MQDs of different ions, and the fluorescence intensity is quenched rapidly within 0.5 min with the addition of Fe^{3+} (Fig. 3a). As can be seen from Fig. 3b, after adding 100 μmol/L Fe^{3+}, the fluorescence decreases significantly and is almost quenched, indicating that N-MQDs have a high detection efficiency for Fe^{3+}. The results show that N-MQD has a strong detection potential for Fe^{3+} [40–42], and the detection limit can be as low as 2 μmol/L (Fig. 3c). In addition, in order to avoid the possible influence of other factors on N-MQDs, interference detection of other metal ions is of great importance. Fig. 3d

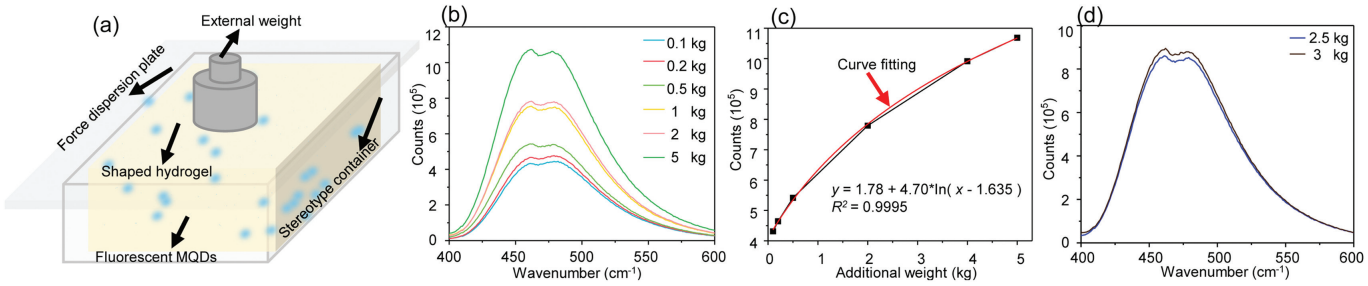

Fig. 4. (a) Schematic diagram of a hydrogel fluorescence emission intensity test; (b) The relationship between the fluorescence intensity of the hydrogel (doped with N-MQDs) and the external force to which the hydrogel was subjected; (c) A fitted curve between the fluorescence intensity of the hydrogel (doped with N-MQDs) and the external force; (d) The relationship between the fluorescence intensity of N-MQDs doped hydrogel and the external force (3 kg; 2.5 kg) to which hydrogel was subjected.

can be seen that, by comparing the fluorescence interference responses of various ions to N-MQDS, other ions basically have no meaning influence on the fluorescence of N-MQDs, except Fe^{3+}. This obvious change in fluorescence intensity can be attributed to the fact that Fe^{3+} promotes electron/hole recombination annihilation through an alternative and effective electron transfer process, which leads to changes in the morphology and electronic state of the N-MQDs surface, and the selectivity of N-MQDs quenching is also the key to eliminating fast response and detection limit [43]. In addition, the changes of fluorescence lifetime and UV–vis absorption of N-MQDs (Fig. S5 in Supporting information) indicate that the presence of Fe^{3+} has no effect on the lifetime absorption, which proves that Fe^{3+} makes the fluorescence quenching of N-MQDs be static quenching. The specificity and selectivity of N-MQDs in Fe^{3+} provide an important contribution to the contemporary role of N-MQDs in heavy ion detection and stress monitoring.

In addition, due to the fluorescence properties of N-MQDs are easy to be oxidized or quenched by extreme environments and metal ions, we developed a fluorescent hydrogel that can enhance the fluorescence intensity. Adding fluorescent quantum dots into hydrogels will expand the application scope of N-MQDs, such as remote mechanical fluorescence monitoring applications [44–46]. In the hydrogel fluorescence force measurement experiment, as shown in Fig. 4a, the hydrogel of the same size is fixed in the foam mold to avoid shape changes and maintain the external force to bear the weight. When the hydrogel is compressed by an external force, the volume of the hydrogel decreases, and the unit volume concentration of fluorescent quantum dots increases, leading to the increase of fluorescence emission intensity of the fluorescent hydrogel, which makes it feasible to monitor the size of external force by the change of fluorescence intensity of the hydrogel. The fluorescence intensity changes to determine the strength of the external force. As shown in Fig. 4b, the fluorescence intensity of hydrogels changed obviously and the detection range is large. Through linear fitting, the relationship between the fluorescence intensity of the fluorescent hydrogel and the external force was obtained (Fig. 4c). In order to verify the reliability of the method, a confirmatory experiment (Fig. 4d) was carried out. The result shows that the external force measured by the hydrogel fluorescence intensity change method is similar to the actual external force, and can correspond to the force value in the fitting curve, which proves that the performance has universal applicability in the application. Therefore, we can realize the perception and calculation of the environmental stress of the material by calculating the fitting curve of the change of the fluorescence intensity on the surface of the remote detection material (fluorescent hydrogel).

In conclusion, we first developed bright blue fluorescent N-MQDs with Ta_4C_3 as the precursor. It showed a very high QY (23.4%) and excellent fluorescence stability. The specificity and selectivity of N-MQDs in the detection of Fe^{3+} make it promising to be a fast and ultra-sensitive fluorescent probe in diverse environmental detection and protection applications. In addition, the accuracy of stress monitoring shown by hydrogel quantum dots has a broad application prospect in optical, mechanical and architectural fields.

Declaration of competing interest

The authors declare that they have no known competing financial interests or personal relationships that could have appeared to influence the work reported in this paper.

Acknowledgments

This research was supported by the National Natural Science Foundation of China (No. 81972901), the Key R & D Plan of Chenzhou (No. ZDYF202008), the Discipline Leader Startup Fund of Huazhong University of Science and Technology Union Shenzhen Hospital (No. YN2021002), Science Foundation of China University of Petroleum, Beijing (Nos. 2462019QNXZ02, 2462019BJRC007).

Supplementary materials

Supplementary material associated with this article can be found, in the online version, at doi:10.1016/j.cclet.2021.11.020.

References

[1] A. Zamhuri, G.P. Lim, N.L. Ma, K.S. Tee, C.F. Soon, Biomed. Eng. Online 20 (2021) 33.
[2] Y.P. Guo, H.S. Wang, X. Feng, et al., Nanotechnology 32 (2021) 195701.
[3] W. Meng, X. Liu, H. Song, et al., Nano Today 40 (2021) 101273.
[4] J.F. Ma, L.Z. Zhang, X. Chen, et al., Chin. Chem. Lett. 32 (2021) 1532–1536.
[5] Y. Liu, J.F. Wei, X. Yan, et al., Chin. Chem. Lett. 32 (2021) 861–865.
[6] B. Kong, C. Selomulya, G. Zheng, D. Zhao, Chem. Soc. Rev. 44 (2015) 7997–8018.
[7] J. Halim, S. Kota, M.R. Lukatskaya, et al., Adv. Funct. Mater. 26 (2016) 3118–3127.
[8] S.J. Xu, D. Li, P.Y. Wu, Adv. Funct. Mater. 25 (2015) 1127–1136.
[9] M. Naguib, M. Kurtoglu, V. Presser, et al., Adv. Mater. 23 (2011) 4248–4253.
[10] W. Qiao, S.M. Yan, X.Y. Song, et al., Appl. Surf. Sci. 359 (2015) 130–136.
[11] Z. Lia, T.Y. Wang, F. Zhu, Z. Wang, Y.W. Li, Chin. Chem. Lett. 31 (2020) 783–786.
[12] S.Y. Lu, L.Z. Sui, Y. Liu, et al., Adv. Sci. 6 (2019) 1801470.
[13] Q. Xu, L. Ding, Y.Y. Wen, et al., J. Mater. Chem. C 6 (2018) 6360–6369.
[14] M. Buzaglo, E. Ruse, I. Levy, et al., Chem. Mater. 29 (2017) 9998–10006.
[15] L.L. Li, J. Ji, R. Fei, et al., Adv. Funct. Mater. 22 (2012) 2971–2979.
[16] Q.Q. Li, S. Zhang, L. Dai, L.S. Li, J. Am. Chem. Soc. 134 (2012) 18932–18935.
[17] Q. Xu, J. Ma, W. Khan, et al., Chem. Commun. 56 (2020) 6648–6651.
[18] Q. Xu, W. Cai, W.K. Li, et al., Mater. Today Energy 10 (2018) 222–240.
[19] X. Chen, X.K. Sun, W. Xu, et al., Nanoscale 10 (2018) 1111–1118.
[20] N. Driscoll, A.G. Richardson, K. Maleski, et al., ACS Nano 12 (2018) 10419–10429.
[21] Q. Xu, Y. Liu, C. Gao, et al., J. Mater. Chem. C 3 (2015) 9885–9893.
[22] M.S. Refat, S.B. Bakare, T. Altalhi, F.R. Hassan, J. Mol. Liq. 328 (2021) 115493.
[23] C.H. Yang, W.X. Que, Y. Tang, Y.P. Tian, X.T. Yin, J. Electrochem. Soc. 164 (2017) 1939–1945.
[24] Q. Xu, W.J. Yang, Y.Y. Wen, et al., Appl. Mater. Today 16 (2019) 90–101.
[25] H. Lin, Y.W. Wang, S.S. Gao, Y. Chen, J.L. Shi, Adv. Mater 30 (2018) 1703284.
[26] H. Lin, Y.W. Wang, S.S. Gao, Y. Chen, J.L. Shi, Adv. Mater. 32 (2020) 1.
[27] M.W. Barsoum, A. Crossley, S. Myhra, J. Phys. Chem. Solids 63 (2002) 2063–2068.

[28] Z.F. Hou, X.L. Wang, T. Ikeda, et al., Phys. Rev. B 85 (2012) 165439.
[29] L. Ding, Y. Wei, L. Li, et al., Nat. Commun. 9 (2018) 155.
[30] A. Darlinski, J. Halbritter, Surf. Interface Anal. 10 (1987) 223–237.
[31] X.F. Z.hang, Y. Guo, Y.J. L.i, Y. Liu, S.L. Dong, Chin. Chem. Lett. 30 (2019) 502–504.
[32] S.J. Zhu, Y.B. Song, X.H. Zhao, et al., Nano Res 8 (2015) 355–381.
[33] N.K. Chaudhari, H. Jin, B. Kim, et al., J. Mater. Chem. A 5 (2017) 24564–24579.
[34] N. Shao, Y. Zhang, S.M. Cheung, et al., Anal. Chem. 77 (2005) 7294–7303.
[35] E.M. Nolan, S.J. Lippard, Chem. Rev. 108 (2008) 3443–3480.
[36] Q.W. Guan, J.F. Ma, W.J. Yang, et al., Nanoscale 11 (2019) 14123–14133.
[37] P. Yang, S. Zhang, X.F. Chen, et al., Mater. Horizons 7 (2020) 746–761.
[38] E.D. Melton, E.D. Swanner, S. Behrens, C. Schmidt, A. Kappler, Nat. Rev. Microbiol. 12 (2014) 797–808.
[39] L. Mezzaroba, D.F. Alfieri, A.N. Colado Simao, E.M.Vissoci Reiche, Neurotoxicology 74 (2019) 230–241.
[40] L. Wang, B.Q. Li, F. Xu, et al., Biomaterials 145 (2017) 192–206.
[41] X. Yan, Y. Song, C.Z. Zhu, et al., Anal. Chem. 90 (2018) 2618–2624.
[42] P. Yang, X. Zhou, J.H. Zhang, et al., Green Chem. 23 (2021) 1834–1839.
[43] A. Ananthanarayanan, X.W. Wang, P. Routh, et al., Adv. Funct. Mater. 24 (2014) 3021–3026.
[44] S. Bhattacharya, R.S. Phatake, S.N. Barnea, et al., ACS Nano 13 (2019) 1433–1442.
[45] M. Li, W.J. Li, W. Cai, et al., Mater. Horizons 6 (2019) 703–710.
[46] P. Yang, F. Zhu, Z.B. Zhang, et al., Chem. Soc. Rev. 50 (2021) 8319–8343.